HHS Public Access

Author manuscript

Biofabrication. Author manuscript; available in PMC 2015 June 01.

Published in final edited form as:

Biofabrication. 2014 June ; 6(2): 024104. doi:10.1088/1758-5082/6/2/024104.

Fabrication of Freestanding Alginate Microfibers and Microstructures for Tissue Engineering Applications

John M Szymanski[1] and **Adam W Feinberg**[1,2]

Adam W Feinberg: Feinberg@andrew.cmu.edu

[1]Department of Biomedical Engineering, Carnegie Mellon University, Pittsburgh, PA 15219, USA

[2]Department of Materials Science and Engineering, Carnegie Mellon University, Pittsburgh, PA 15213, USA

Abstract

Natural biopolymers such as alginate have become important materials for a variety of biotechnology applications including drug delivery, cell encapsulation and tissue engineering. This expanding use has spurred the development of new approaches to engineer these materials at the nano- and microscales to better control cell interactions. Here we describe a method to fabricate freestanding alginate-based microfibers and microstructures with tunable geometries down to approximately 3 μm. To do this, a polydimethylsiloxane (PDMS) stamp is used to micromold alginate or alginate-fibrin blends onto a sacrificial layer of thermally-sensitive poly(N-isopropylacrylamide) (PIPAAm). A warm calcium chloride solution is then used to crosslink the alginate and upon cooling below the lower critical solution temperature (~32° C) the PIPAAm layer dissolves and releases the alginate or alginate-fibrin as freestanding microfibers and microstructures. Proof-of-concept experiments demonstrate that C2C12 myoblasts seeded onto the alginate-fibrin microfibers polarize along the fiber length forming interconnected cell strands. Thus, we have developed the ability to engineer alginate-based microstructured materials that can selectively bind cells and direct cellular assembly.

1. Introduction

Naturally-derived biopolymers are used in a variety of biotechnology applications including drug delivery [1-3], cell encapsulation [4-6], wound dressings [7, 8], and as tissue engineering scaffolds [9-11]. Alginate is commonly used because it is a linear polysaccharide that can be derived in large quantities from algae, yet is similar to the glycosaminoglycans found in the extracellular matrix (ECM) in animals. Specifically, alginate is hydrophilic, has low immunogenicity, is non-toxic, and can be crosslinked in the presence of divalent cations, such as calcium, to form hydrogels [12, 14], microparticles [15], and fibers [9, 10, 16]. These properties have led to the use of alginate-based materials for the regeneration of skin [17, 18], cartilage [19, 20], and bone tissue [20-22]. Additionally, alginate can be easily modified to tune mechanical properties [23] or engineered with defined surface topographies to direct cell behavior [24]. Incorporating micro- and nanoscale topographical and chemical patterning is particularly important because features over this spatial range enable these materials to further mimic the composition and architecture of the ECM in tissues and influence a variety of processes [25]

such as cell adhesion [26, 27], alignment [28, 29], and migration [30]. Thus, microscale engineering of alginate has the potential to improve the ability of these biomaterials to control cell behavior in tissue engineering applications.

To date, researchers have developed a number of approaches to create micro- and nanoscale alginate fibers and structures. For example, coaxial flow based microfluidic devices [16, 31] and electrospinning [9, 10] techniques have established the ability to fabricate alginate fibers with micro- and nanoscale diameters, respectively. While these methods can create fibrous scaffolds for either cell encapsulation [31] or cell growth [9, 10], they are limited by the number of possible fiber geometries and orientations. Greater geometrical control can be achieved through the use of micromolding techniques with poly(dimethylsiloxane) (PDMS) stamps, which has been used to fabricate microstructured hydrogels out of materials such as hyaluronic acid [6], chitosan [32], and poly(ethylene glycol) [33]. Topographically patterned alginate has also been formed using microfabricated agarose stamps loaded with $CaCl_2$ to form crosslinks [24, 34]. These micromolded alginate structures are typically tens to hundreds of micrometers in thickness, and thus have sufficient mechanical strength to be manually removed from the surface they were molded on. However, alginate structures on the order of a few micrometers in thickness, particularly those with a high surface area to volume ratio, are difficult to remove without damaging them.

We hypothesized that by combining micromolding with a sacrificial release surface we could fabricate geometrically well-defined, freestanding alginate fibers and structures at the micrometer scale. To test this we modified a fiber fabrication approach termed surface-initiated assembly (SIA) [35], which can produce freestanding ECM protein nanofibers and nanostructures. We found that the PDMS stamps originally used in SIA for microcontact printing could instead be used as micromolds to pattern alginate and alginate-fibrinogen blends on a thermally sensitive, poly(N-isopropylacrylamide) (PIPAAm) surface. Physiologic levels of $CaCl_2$ are sufficient to crosslink the micromolded alginate and temperature can be controlled to dissolve the sacrificial PIPAAm layer once fiber formation is complete. The geometry of the alginate fibers and structures is easily tuned by modifying the topography of the PDMS stamp used for micromolding. Furthermore, by micromolding blends of alginate and fibrinogen we can engineer microfibers that support cell adhesion and direct uniaxial cell alignment.

2. Results

2.1 Fabricating freestanding alginate microfibers

We developed a method to engineer microfibers and microstructures from alginate using a micromolding technique in combination with a thermally sensitive release surface. This is similar to previously published work on the SIA of ECM proteins, except instead of microcontact printing ECM proteins onto a surface, the PDMS stamp was used as a micromold. The basic process is illustrated in Figure 1 using the example of alginate fibers, but essentially any design that can be engineered into the PDMS stamp can be generated. Briefly, a glass coverslip was spincoated with PIPAAm and placed on top of a hotplate set to 45 °C to prevent dissolution of the thermally sensitive PIPAAm layer. A 10 μL drop of 2% alginate dissolved in DI water was then placed on top of the PIPAAm (Figure 1a).

Immediately, a topographically patterned PDMS stamp was pressed onto the PIPAAm-coated glass coverslip, displacing the alginate solution (Figure 1b), and heated until the alginate was completely dry. Next, the PDMS stamp was removed, leaving behind dried alginate fibers on the PIPAAm surface corresponding to the negative pattern of the PDMS stamp (Figure 1c). To release the alginate fibers from the PIPAAm surface, a 2% $CaCl_2$ solution at 40 °C was added (Figure 1d). Cooling below the lower critical solution temperature of the PIPAAm (~32 °C) triggered its hydration and dissolution, which subsequently released the Ca^{2+} crosslinked, insoluble alginate fibers from the surface (Figure 1e). Micromolded polysaccharides are typically used for cell encapsulation applications [5, 6, 34], but we sought to leverage our approach to create microstructured scaffolds that were also cell adhesive. Previous work has shown that alginate can be modified with RGD peptides [9, 36, 37], growth factors [20], or blended with fibrin [38] or collagen [39, 40] in order to bind cells. Based on this work, we blended the 2% alginate solution with 20 mg/mL fibrinogen (Figure 1a) and then added 10 units/mL of thrombin to the $CaCl_2$ release solution to crosslink the fibrinogen into fibrin. This approach creates a composite alginate-fibrin hydrogel that can be micromolded in the same way as the 100% alginate.

Releasing crosslinked alginate microfibers from the surface requires both the $CaCl_2$ in solution to crosslink the alginate as well as the thermally-sensitive PIPAAm layer to enable non-destructive release. For example, alginate fibers, 30 μm wide and 1 cm long, were micromolded onto a glass surface without the PIPAAm layer, and while able to crosslink in a 2% $CaCl_2$ solution, they remained permanently bound to the surface, even after 12 hours (Figure 2a). While thicker alginate structures on the millimeter scale might be able to be peeled off the glass surface, the micrometer-thick fibers we engineered were too fragile. Therefore, a release surface was necessary to non-destructively release the alginate microfibers. While there are other materials that can potentially be used besides PIPAAm, our previous work has demonstrated the ability to use PIPAAm to nondestructively release delicate ECM protein fibers only 10 nm thick. As expected, $CaCl_2$ was also necessary to crosslink the alginate microfibers that were on the PIPAAm surface. Rehydrating with 40 °C DI water without $CaCl_2$ failed to form alginate fibers upon dissolution of PIPAAm, and the alginate simply dissolved into solution (Figure 2b). We then evaluated a high and low concentration of $CaCl_2$ and showed that a 0.5% w/v (Figure 2c) and 2% w/v (Figure 2d) were capable of achieving fiber formation. While we did not observe any structural differences as a function of $CaCl_2$ concentration, previous work in the literature suggests that the elastic modulus can be tuned with $CaCl_2$ concentrations from 10 to 100 mM (0.15% to 1.5% w/v) to give elastic moduli of 4 to 60 kPa [24]. Further investigation is needed to determine how $CaCl_2$ concentration affects structural and mechanical properties of the freestanding, microscale alginate fibers we have engineered.

2.2 Alginate microfiber morphology pre- and post-release

To morphologically characterize the alginate microfibers we used confocal microscopy to measure the width and thickness both pre-release and post-release. Alginate was fluorescently labeled and micromolded to form 20 μm (Figure 3a) and 50 μm (Figure 3f) wide fibers. Upon crosslinking and thermally triggered release, both alginate microfibers

noticeably decreased in their width (Figure 3b and 3g). Generating a cross-sectional view from the confocal 3D image demonstrated that the thickness of the microfibers was uniform (Figure 3c and 3h). Interestingly, a thin layer of alginate was visible between the fibers, but did not crosslink upon release, suggesting there is a minimum thickness for fiber formation. Quantitatively, alginate microfibers initially 19.71 ± 0.19 μm in width pre-release decreased to 5.45 ± 2.58 μm in width post-release (Figure 3d, n=40, $P<0.01$). Similarly, alginate microfibers initially 50.00 ± 0.22 μm in width decreased to 15.79 ± 10.42 μm in width post-release (Figure 3i, n=40, $P<0.01$). Thus, for both the 20 and 50 μm wide fibers, the width decreased ~70% upon release from the PIPAAm. The pre-release thickness of 20 μm (Figure 3c) and 50 μm (Figure 3h) wide alginate microfibers was 2.72 ± 0.17 μm and 2.96 ± 0.21 μm, respectively (n = 12 for both). Upon thermally triggered release, the thickness of the 20 μm and 50 μm wide alginate fibers increased to 3.48 ± 0.61 μm (Figure 3e, n = 12) and 4.00 ± 0.51 μm (Figure 3j, n=12), respectively. This corresponds to a ~70% decrease in width and a ~30% increase in thickness, which we attributed to the hydration of the alginate once it was no longer confined to a specific shape by adhesion to the underlying PIPAAm surface. Because the microfibers were very long, we were unable to quantify changes in length. However, confocal analysis did show that we were capable of engineering alginate microfibers where the thickness and width were well defined by the depth and spacing of the features in the PDMS stamp, respectively.

2.3 Fabricating complex alginate microstructures

In addition to microfibers, we also fabricated a variety of complex alginate microstructures by changing the features on the PDMS stamp used as the mold. For example, we fabricated alginate sheets with well-defined, 75 μm wide square pores (Figure 4a). After hydration in 2% $CaCl_2$ and thermally triggered release from the PIPAAm surface, the fidelity and spatial arrangement of the pores remained intact. Similarly, we also fabricated a sheet of alginate with 50 μm-wide circular pores that also maintained their fidelity and spatial arrangement upon release in 2% $CaCl_2$ solution (Figure 4b). Thus, by adjusting the topography of the PDMS stamp, alginate sheets with well-defined pore size, spacing, geometry and arrangement can be easily fabricated. We were also able to fabricate complex, freestanding alginate microstructures. As proof-of-concept, we fabricated multi-armed alginate stars where each arm was 100 μm in length and 20 μm in width (Figure 4c). Similar to the aforementioned alginate fibers and porous sheets, the star patterns could be micromolded onto the PIPAAm surface with high pattern fidelity. The alginate stars also retained their morphology after release in 2% $CaCl_2$ solution. While some of the star patterns managed to fold over themselves, they still maintained their initial micromolded geometry. Thus, it is evident that a variety of complex shapes and structures can be fabricated and released from the surface using our approach. With recent advances in photolithographic processes it is possible to fabricate PDMS stamps with features on a submicron level; potentially enabling the fabrication of extremely complex and intricate alginate microstructures, or even nanostructures. However, the failure of submicron thick alginate films to crosslink (see area between fibers in Figure 3c and 3h) suggests there is a lower limit for there to be enough alginate to crosslink effectively. Further investigation is needed to determine the resolution limits of what can effectively be micromolded, crosslinked and released while retaining fidelity and structural integrity.

2.4 Fabrication of alginate-fibrin fibers to control cell adhesion and alignment

While alginate has gained popularity for a variety of biomedical applications ranging from drug delivery to cell encapsulation, a limitation of this material for tissue engineering is the inability of cells and serum proteins to bind/adsorb [13]. One option is to covalently modify the alginate with polypeptide sequences to add bioactivity, such as the RGD amino acid sequence to bind cell surface integrins [9, 36]. However, we chose to simply blend the alginate with an ECM protein, in this case fibrinogen, which has been shown previously to increase cell adhesion to bulk alginate scaffolds [38]. We combined 20 mg/ml alginate solution with 20 mg/ml fibrinogen and then micromolded it as described for the pure alginate microfibers. We found that higher concentrations of fibrinogen prevented good pattern fidelity due to premature crosslinking and formation of a fibrin gel on the PIPAAm surface prior to micromolding (data not shown). To crosslink and release the microfibers we used a 2% $CaCl_2$ solution mixed with 10 units/mL thrombin to catalyze the conversion of fibrinogen to fibrin [41]. Note that for alginate-fibrin blends we decreased the hotplate temperature from 45 °C to 40 °C to avoid thermal denaturing of the fibrinogen.

We analyzed the morphology of alginate-fibrin microfibers in a dry, pre-release state and a hydrated, post-release state using confocal microscopy in order to determine changes in width and thickness (Figure 5a and 5b). Unlike the pure alginate fibers that had a uniform appearance, the alginate-fibrin microfibers had a speckled appearance that we interpreted as phase separation into alginate and fibrin rich domains within the microfiber. The ability to release intact microfibers indicated that the alginate-fibrin blends maintained structural integrity during the release process. However, unlike the pure alginate microfibers that underwent large dimensional changes upon hydration and release (Figure 3b, g), the released alginate-fibrin microfibers had a morphology that was closer to the pre-release state. Consistent with the results for the alginate microfibers, cross-sections from the 3D confocal images demonstrated that the thickness of the alginate-fibrin microfibers was uniform (Figure 5c). Quantitative analysis showed the alginate-fibrin microfibers initially 30.48 ± 0.94 μm in width pre-release decreased to of 24.10 ± 5.44 μm in width post-release (Figure 5d, $n = 29$, $P<0.01$). This ~20% decrease in width is much smaller than the ~70% decrease in width we observed with pure alginate microfibers, suggesting the presence of cross-linked fibrin may limit the alginate from changing shape during release. The thickness of the alginate-fibrin microfibers was initially 3.14 ± 0.29 μm pre-release and increased to 3.96 ± 0.25 μm post-release (Figure 5e, $n = 11$, $P<0.01$), a ~30% increase in thickness and similar to the increase observed with pure alginate microfibers. Thus, the presence of cross-linked fibrin altered the morphological changes associated with hydration and release.

Next, we evaluated the stability of the alginate-fibrin microfibers under cell culture conditions with and without cells and tested their ability to support cell adhesion. We chose to conduct these experiments using alginate and alginate-fibrin microfibers micromolded directly onto glass coverslips because this immobilized the fibers and facilitated microscopic observation over a multiday time period. First, we investigated the stability of the alginate and alginate-fibrin microfibers in media in a cell culture incubator over 5 days (Figure 6a and 6b). As expected, in both cases the microfibers maintained their morphology, an indication that these microfibers were not susceptible to hydrolysis over this time period.

Second, we seeded alginate (Figure 6c) and alginate-fibrin (Figure 6d) microfibers with C2C12 cells and cultured them for 5 days. C2C12s did not adhere to the pure alginate microfibers and instead adhered to the glass surface between microfibers, despite being pretreated with Pluronics F127 (Figure 6c). The cells were able to proliferate and after 3 days, at regions of high cell density, were able to migrate across the microfibers. However, even after 5 days in culture the C2C12s did not adhere directly to the alginate microfibers, which via fluorescent imaging remained intact and predominantly served as topographical barriers that promoted cell alignment parallel to the length of the microfibers. In contrast, C2C12s seeded onto the alginate-fibrin microfibers were able to initially adhere and align along the length of the microfibers (Figure 6d). By day 3, the cells began to bridge between parallel microfibers and by day 5, fluorescent imaging confirmed that the cells began to degrade the alginate-fibrin microfibers. While there was a general overall alignment of the cells in the direction the microfibers were initially oriented, alginate-fibrin microfibers had clearly degraded to the point where some cells were no longer using them as a guidance cue. These results confirmed that the fibrin component of the microfibers was active as a cell binding moiety and at sufficient density to support cell adhesion. Further, the fibrin was also susceptible to cell-mediated degradation and by 5 days had mostly detached from the glass, undergone substantial morphological changes and appeared to break apart in places. Further investigation is needed to determine how fibrinogen concentration in the precursor solution affects the adhesivity and degradation rate of the microfibers and how much this can be tuned.

Next, we evaluated whether the alginate-fibrin microfibers were capable of supporting cell adhesion as free-standing scaffolds. First, as a control, we micromolded alginate microfibers on PIPAAm, seeded C2C12 cells, cultured them for 12 hours and then released the microfibers (Figure 7a). By doing this the microfibers remained attached to the surface during seeding and cell culture, simplifying microscopic evaluation. As expected, even after 12 hours in culture, the cells were unable to adhere to the alginate microfibers and when released we did not observe any adherent cells to the free-standing microfibers. Next, we repeated the experiment using alginate-fibrin microfibers and after 12 hours in culture, we released the microfibers from the surface. Using fluorescent imaging of the cell nuclei and actin filaments we confirmed that cells adhered to the alginate-fibrin microfibers and remained adhered after thermally triggered release (Figure 7b). This is important, because the alginate-fibrin microfibers undergo changes in width and thickness that could potentially disrupt cell adhesion (Figure 5d and 5e). Examining cells adhered to a single alginate-fibrin microfiber clearly showed that they were aligned along the length of the microfiber, with the potential to form a nearly continuous cell strand (Figure 7c). It was also possible to engineer an array of parallel alginate-fibrin microfibers with adhered cells by creating a peripheral frame that held all the microfibers in position (Figure 7d). This resulted in a large number of cells aligned on parallel microfibers, a useful structure for the potential of engineering of aligned skeletal muscle tissue from these myoblasts.

While the C2C12 cells were observed to adhere and align onto the alginate-fibrin microfibers after a culture period of 12 hours, Figure 6 suggested that longer culture times may lead to the degradation of the fibers and loss of alignment. Thus, we also investigated stability of the alginate-fibrin microfibers after a longer culture time of 3 days. Fluorescent

imaging indicated that some degradation of the microfibers had occurred, but they still released as continuous fibers (Figure 7e and 7g). Fluorescent imaging of the bound cells revealed robust attachment and alignment in the fiber direction (Figure 7f and 7h). This alignment appeared better than for C2C12 cells seeded on the alginate-fibrin microfibers micromolded on glass (Figure 6d) and may be due to the PIPAAm surface being a better repellent of cell adhesion than the Pluronics-treated glass surface. These experiments confirmed that the alginate-fibrin microfibers could be used to engineer a free-standing network of aligned cells. Further studies will be needed to determine how adhesivity and degradation can be modulated by adjusting the concentration of fibrinogen in the precursor solution, with a near term goal of maximizing and maintaining alignment long enough for the C2C12 myoblasts to fuse into contractile myotubes.

3. Discussion

The ability of micro- and nanoscale structures and topographies to influence cell function has led to the emergence of new methods to fabricate alginate materials on these scales for tissue engineering [23, 25] and drug delivery applications [23, 42]. Here we have developed a method to engineer freestanding alginate and alginate-fibrin microfibers and microstructures with tunable planar dimensions and a thickness on the order of ~3-4 μm. The unique aspect of this work is the micromolding in combination with the PIPAAm release surface, which enables very thin and delicate structures to be released nondestructively. Further, the micromolding enables high fidelity and high uniformity of the engineered structures. An advantage of this approach over electrospun alginate fibers is the fact that we do not need to incorporate additives such as poly(ethylene glycol) [9, 10] or poly(vinyl alcohol) [43]. Previous work in the literature has demonstrated the ability to fabricate micromolded alginate and other hydrogel structures for cell encapsulation [5, 6, 34]. However, these alginate structures are generally on the order of tens to hundreds of micrometers in thickness and can be manually harvested off of the PDMS substrate they were micromolded on. In contrast, alginate structures with thicknesses of <10 μm are more difficult to remove due to the higher surface area and greater, non-specific interfacial adhesion. For example, alginate microfibers formed directly on glass did not release (Figure 2a) over a 12 hour period. Attempts to manually remove the microfibers from the glass surface served to disrupt the pattern fidelity and clearly broke some of the alginate microfibers (data not shown). Further, when cells are bound to the alginate-fibrin microfibers mechanical damage to the cell, from excessive strain during attempted removal, becomes an even greater concern. Thus, the use of the sacrificial PIPAAm layer is critical for the nondestructive release of the assembled alginate microfibers and microstructures from the surface, both with and without cells.

For freestanding alginate microfibers and microstructures to serve as scaffolds for tissue engineering applications, the alginate needs to be modified in order to support cell adhesion [13]. One approach to do this has been to covalently modify the alginate to contain the RGD cell adhesion peptide [9, 36, 37]. This has been shown to enhance cell adhesion but incorporates only a single type of integrin binding site, which is only one part of the biofunctionality of full length ECM proteins [44]. For example, the RGD peptide sequence on the tenth, type III repeat unit of fibronectin is neighbored by the proline-histidine-serine-

arginine-asparagine (PHSRN) synergy site on the ninth, type III repeat. The juxtaposition of these two domains promotes $\alpha_5\beta_1$ integrin adhesion whereas the RGD sequence alone promotes adhesion via the $\alpha_v\beta_3$ integrin [45, 46]. Binding of different integrins has been shown to promote different downstream cell responses such as epithelial-to-mesenchymal transition in alveolar epithelial cells [47]. Alginate has recently been modified with both the PHSRN and RGD peptide sequences, which has been shown to improve the differentiation of normal human osteoblasts [48]. However, adding small peptide sequences to alginate is limited in the total number of moieties that can be integrated. Integration of full-length ECM proteins has been achieved using alginate-fibrin [38] and alginate-collagen [39, 40] composite hydrogels, and using streptavidin functionalized alginate to bind to biotinylated ECM proteins [24]. Here we chose to incorporate fibrinogen into the alginate precursor solution because it is an established and straightforward way to introduce cell binding sites into the microfibers (Figures 6 and 7). Further, fibrin is biodegradable via cell-secreted enzymes and thus provides a substrate that can be remodeled by the cells. This is indeed what we observed when cells were cultured on alginate-fibrin microfibers over a prolonged period of time (Figure 6d and 7e to 7h). It should be noted that the alginate-fibrin microfibers we engineered initially had widths previously shown to be able to uniaxially align adhered muscle cells [49]. This was precisely what we observed during short culture periods of 12 hours (Figures 7b to 7d), but over multiple days, the cells were able to degrade the fibers and the degree of guidance decreased (7e to 7h). Because the degradation was due to cell-mediated remodeling and not hydrolysis, it is conceivable that by tuning the concentration of fibrinogen, the amount of thrombin and/or using aprotinin that we can also tune the degradation rate of the fibers.

The micromolding and PIPAAm release approach described in this paper is also more broadly applicable to other biopolymers and compositions. For example, while we only investigated a single concentration of fibrinogen in our alginate-fibrin microfibers, we anticipate that a wider range is possible, which would enable tuning of the cell adhesivity and biodegradation characteristics [50, 51]. Further, other ECM proteins such as collagen type I [52] or Matrigel [53] could be blended with the alginate to form composite hydrogels. In these cases, physiologic temperature could be used to trigger gelation, rather than the thrombin used for the fibrin. More complicated combinations are also possible by blending multiple ECM proteins with other bioactive molecules such as growth factors. For example, it is conceivable that fibronectin could be mixed in with an alginate-collagen blend and then platelet-derived growth factor (PDGF) could be immobilized on the scaffold by binding to the fibronectin [54]. Future work will focus on expanding the materials that can be used in this micromolding technique and applying it to a variety of tissue engineering applications. Specifically, we will build upon the preliminary work using C2C12 myoblasts adhered to alginate-fibrin microfibers (Figure 7) by differentiating the cells into myotubes and creating ‘muscular threads’ that we can engineer into functional muscle tissue constructs.

4. Conclusion

We have developed a method to fabricate alginate and alginate-fibrin microfibers and microstructures using a micromolding technique in combination with a nondestructive release surface. Proof-of-concept was demonstrated by engineering freestanding structures

with tunable planar (XY) dimensions and a thickness of <5 μm. Scaffolds of assembled alginate microfibers were easily manipulated upon release suggesting a range of potential biomedical applications. By fabricating alginate-fibrin microfibers, this approach leveraged the bioactive properties of ECM proteins in a microstructured material to promote cell adhesion and alignment on a freestanding scaffold. Future work will expand this technology by exploring the tunability of the system. Specifically, we will investigate how $CaCl_2$ concentration affects the mechanical properties of the alginate microfibers in order to tune the elastic modulus. This would lead to alginate-based microfibers and microstructure where, by blending with other ECM proteins, we would be able to engineer the geometrical, topographical, biochemical, and mechanical properties for potential use in a wide range of tissue engineering applications.

5. Methods

5.1 Fabrication of freestanding alginate microfibers and microstructures

The microfabricated PDMS stamps used to micromold the alginate and alginate-fibrin blends were prepared using photolithography, similar to previously published procedures [35, 55]. Briefly, glass wafers were spincoated with SPR 220.3 positive photoresist (Microchem) and exposed to UV light through a transparency-based photomask. Exposed regions were removed using MF-319 developer (Microchem) leaving behind a glass wafer with a microtopographically patterned photoresist layer on top. Sylgard 184 PDMS (Dow Corning) was mixed in a 10:1 base to curing agent ratio, degassed and then cast over the microfabricated wafers and cured for a minimum of 4 hours at 65 °C. The PDMS was then peeled off the wafers and cut into 1.5 cm^2 stamps. Prior to use, the PDMS stamps were sonicated in a 50% ethanol solution to remove contaminants and then dried under a stream of nitrogen.

Alginate microfibers and microstructures were fabricated using micromolding with the PDMS stamps. First, a PIPAAm coated 25 mm diameter glass coverslip was prepared by spincoating a 10% PIPAAm (Polysciences Inc) in a 1-butanol (w/v) solution. Next a 10 μL droplet of 2% (w/v, g/mL) sodium alginate (FMC Biopolymer) in DI water was pipetted onto the PIPAAm coated glass coverslip. A microfabricated PDMS stamp was then pressed onto the alginate droplet (Figure 1a) and into conformal contact with the PIPAAm surface. To prevent premature dissolution the PIPAAm coated coverslips, PDMS stamps, and alginate solution were pre-heated to 40 °C in an oven and all micromolding took place on top of a hot plate set to 45 °C. The PDMS stamp was kept in conformal contact until the alginate solution had dried, typically 2-3 hours (Figure 1b). Once dried, the PDMS stamp was removed (Figure 1c) and the fidelity of the micromolded alginate microfibers and microstructures were inspected using phase contrast microscopy. The alginate features were released by hydration in 40 °C $CaCl_2$ (Sigma-Aldrich) solution with concentrations ranging between 0.5-2% (w/v) (Figure 1d). Allowing the solution to cool below the LCST resulted in the dissolution of PIPAAm and the release of assembled alginate microfibers and microstructures (Figure 1e). To fabricate alginate-fibrin microfibers we mixed 20 mg/mL of fibrinogen with 20 mg/mL of fluorescently labeled alginate. This solution was micromolded and dried as described for pure alginate. To crosslink and release the alginate-fibrin

microfibers we used a 40 °C, solution of 2% w/v $CaCl_2$ and 10 units/ml thrombin. The thrombin catalyzed the conversion of fibrinogen to fibrin enabling the release of freestanding, assembled alginate-fibrin microfibers.

5.2 Characterization of alginate microfiber morphology

Fluorescently-labeled alginate and alginate-fibrin microfibers were imaged using confocal microscopy to measure the width and thickness before and after release from the surface. The alginate was fluorescently labeled based on published protocols [56]. Briefly, 2% w/v alginate solution was combined with 5.68 mM 6-aminofluorescein, 11.36 mM 1-ethyl-3-(3-dimethylaminopropyl) carbodiimide hydrochloride, and 11.36 mM N-hydroxysulfosuccinimide sodium salt (Sigma-Aldrich) and stirred for 48 hours. The solution was then dialyzed to remove unreacted 6-aminofluorescein and the alginate, with ~1/20 of the available carboxylic groups fluorescently-labeled, was stored at 4 °C and protected from light. The fluorescently-labeled alginate and alginate-fibrin microfibers were imaged at 20x and 63x using confocal microscopy (LSM 700, Zeiss) to acquire 2D images and 3D image z-stacks. The images were imported into ImageJ (National Institutes of Health) [57] for quantitative analysis, using the 20x magnification images to measure the width of the alginate microfibers and the orthogonal cross-sections of the 63x z-stacks to measure the thickness of the microfibers. The Mann-Whitney Rank Sum Test with statistical significance based on $P<0.01$ was used for all statistical comparisons (Sigma Plot, Systat Software Inc).

5.4 Cell Culture, Seeding and Fluorescent Staining

The murine C2C12 myoblast cell line (CRL-1722, ATCC) was cultured according to published methods [55]. Briefly, cells were grown in culture media consisting of Dulbecco's Modified Eagle Medium supplemented with 10% fetal bovine serum, 1% L-glutamine (200 mM), 1% 10,000 unit penicillin-streptomycin solution. For experiments, 1×10^5 cells suspended in media were seeded on the different experimental conditions and cultured for 12 hours, 3 days, or 5 days (Figure 6). When seeding on the PIPAAm-coated coverslips all of the solutions were warmed to 37 °C to prevent premature dissolution of the PIPAAm layer. After 12 hours, 3 days or 5 days of culture samples without PIPAAm were fixed in 4% formaldehyde (Polysciences Inc) for 15 min and then washed 3 times in PBS. For samples with PIPAAm the temperature of the solution was allowed to cool below 32 °C to dissolve the PIPAAm layer and release the alginate or alginate-fibrin microfibers. After thermally triggered release, the cells were similarly fixed in 4% formaldehyde. All samples with cells were incubated for 1 hour with a 200 μL solution of PBS containing 1 μL of DAPI and 2 μL Phalloidin conjugated to Alexa-Flour 635 (Invitrogen) to stain for cell nuclei and actin filaments, respectively. The samples were then washed three times in PBS and then mounted with a drop of Prolong Gold antifade reagent (Invitrogen) on microscope glass slides. The mounted samples were stored at room temperature and protected from light for 12 hours to allow the Prolong reagent to cure.

Acknowledgments

We acknowledge financial support from the Biomechanics in Regenerative Medicine NIH T32 Training Program (2T32EB003392) to J.M.S. and the NIH Director's New Innovator Award (1DP2HL117750) to A.W.F.

References

1. Peppas NA, Hilt JZ, Khademhosseini A, Langer R. Hydrogels in Biology and Medicine: From Molecular Principles to Bionanotechnology. Advanced Materials. 2006; 18:1345–60.
2. Chen S-C, Wu Y-C, Mi F-L, Lin Y-H, Yu L-C, Sung H-W. A novel pH-sensitive hydrogel composed of N,O-carboxymethyl chitosan and alginate cross-linked by genipin for protein drug delivery. Journal of Controlled Release. 2004; 96:285–300. [PubMed: 15081219]
3. Luo Y, Kirker KR, Prestwich GD. Cross-linked hyaluronic acid hydrogel films: new biomaterials for drug delivery. Journal of Controlled Release. 2000; 69:169–84. [PubMed: 11018555]
4. Tan WH, Takeuchi S. Monodisperse alginate hydrogel microbeads for cell encapsulation. Advanced Materials. 2007; 19:2696–701.
5. Yeh J, Ling Y, Karp JM, Gantz J, Chandawarkar A, Eng G, Blumling J Iii, Langer R, Khademhosseini A. Micromolding of shape-controlled, harvestable cell-laden hydrogels. Biomaterials. 2006; 27:5391–8. [PubMed: 16828863]
6. Khademhosseini A, Eng G, Yeh J, Fukuda J, Blumling J, Langer R, Burdick JA. Micromolding of photocrosslinkable hyaluronic acid for cell encapsulation and entrapment. Journal of Biomedical Materials Research Part A. 2006; 79A:522–32. [PubMed: 16788972]
7. Boateng JS, Matthews KH, Stevens HNE, Eccleston GM. Wound healing dressings and drug delivery systems: A review. Journal of Pharmaceutical Sciences. 2008; 97:2892–923. [PubMed: 17963217]
8. Xu H, Ma L, Shi H, Gao C, Han C. Chitosan–hyaluronic acid hybrid film as a novel wound dressing: in vitro and in vivo studies. Polymers for Advanced Technologies. 2007; 18:869–75.
9. Jeong SI, Krebs MD, Bonino CA, Khan SA, Alsberg E. Electrospun Alginate Nanofibers with Controlled Cell Adhesion for Tissue Engineeringa. Macromolecular Bioscience. 2010; 10:934–43. [PubMed: 20533533]
10. Bhattarai N, Li Z, Edmondson D, Zhang M. Alginate-based nanofibrous scaffolds: Structural, mechanical, and biological properties. Advanced Materials. 2006; 18:1463–7.
11. Matthews JA, Wnek GE, Simpson DG, Bowlin GL. Electrospinning of Collagen Nanofibers. Biomacromolecules. 2002; 3:232–8. [PubMed: 11888306]
12. Mano JF, Silva GA, Azevedo HS, Malafaya PB, Sousa RA, Silva SS, Boesel LF, Oliveira JM, Santos TC, Marques AP, Neves NM, Reis RL. Natural origin biodegradable systems in tissue engineering and regenerative medicine: present status and some moving trends. Journal of The Royal Society Interface. 2007; 4:999–1030.
13. Augst AD, Kong HJ, Mooney DJ. Alginate Hydrogels as Biomaterials. Macromolecular Bioscience. 2006; 6:623–33. [PubMed: 16881042]
14. Kuo CK, Ma PX. Ionically crosslinked alginate hydrogels as scaffolds for tissue engineering: part 1. Structure, gelation rate and mechanical properties. Biomaterials. 2001; 22:511–21. [PubMed: 11219714]
15. Fundueanu G, Nastruzzi C, Carpov A, Desbrieres J, Rinaudo M. Physico-chemical characterization of Ca-alginate microparticles produced with different methods. Biomaterials. 1999; 20:1427–35. [PubMed: 10454015]
16. Su J, Zheng Y, Wu H. Generation of alginate microfibers with a roller-assisted microfluidic system. Lab on a Chip. 2009; 9:996–1001. [PubMed: 19294313]
17. Hashimoto T, Suzuki Y, Tanihara M, Kakimaru Y, Suzuki K. Development of alginate wound dressings linked with hybrid peptides derived from laminin and elastin. Biomaterials. 2004; 25:1407–14. [PubMed: 14643615]
18. Lee W-R, Park J-H, Kim K-H, Kim S-J, Park D-H, Chae M-H, Suh S-H, Jeong S-W, Park K-K. The biological effects of topical alginate treatment in an animal model of skin wound healing. Wound Repair and Regeneration. 2009; 17:505–10. [PubMed: 19527480]
19. Alsberg E, Anderson KW, Albeiruti A, Rowley JA, Mooney DJ. Engineering growing tissues. Proceedings of the National Academy of Sciences. 2002; 99:12025–30.
20. Re'em T, Witte F, Willbold E, Ruvinov E, Cohen S. Simultaneous regeneration of articular cartilage and subchondral bone induced by spatially presented TGF-beta and BMP-4 in a bilayer affinity binding system. Acta biomaterialia. 2012; 8:3283–93. [PubMed: 22617742]

21. Alsberg E, Anderson K, Albeiruti A, Franceschi R, Mooney D. Cell-interactive alginate hydrogels for bone tissue engineering. Journal of dental research. 2001; 80:2025–9. [PubMed: 11759015]
22. Li Z, Ramay HR, Hauch KD, Xiao D, Zhang M. Chitosan–alginate hybrid scaffolds for bone tissue engineering. Biomaterials. 2005; 26:3919–28. [PubMed: 15626439]
23. Lee KY, Mooney DJ. Alginate: Properties and biomedical applications. Progress in Polymer Science. 2012; 37:106–26. [PubMed: 22125349]
24. Agarwal A, Farouz Y, Nesmith AP, Deravi LF, McCain ML, Parker KK. Micropatterning Alginate Substrates for In Vitro Cardiovascular Muscle on a Chip. Advanced Functional Materials. 2013
25. Dvir T, Timko BP, Kohane DS, Langer R. Nanotechnological strategies for engineering complex tissues. Nature nanotechnology. 2010; 6:13–22.
26. Rho KS, Jeong L, Lee G, Seo B-M, Park YJ, Hong S-D, Roh S, Cho JJ, Park WH, Min B-M. Electrospinning of collagen nanofibers: Effects on the behavior of normal human keratinocytes and early-stage wound healing. Biomaterials. 2006; 27:1452–61. [PubMed: 16143390]
27. Keun Kwon I, Kidoaki S, Matsuda T. Electrospun nano- to microfiber fabrics made of biodegradable copolyesters: structural characteristics, mechanical properties and cell adhesion potential. Biomaterials. 2005; 26:3929–39. [PubMed: 15626440]
28. Bettinger CJ, Zhang Z, Gerecht S, Borenstein JT, Langer R. Enhancement of In Vitro Capillary Tube Formation by Substrate Nanotopography. Advanced Materials. 2008; 20:99–103. [PubMed: 19440248]
29. Yang F, Murugan R, Wang S, Ramakrishna S. Electrospinning of nano/micro scale poly(l-lactic acid) aligned fibers and their potential in neural tissue engineering. Biomaterials. 2005; 26:2603–10. [PubMed: 15585263]
30. Diehl KA, Foley JD, Nealey PF, Murphy CJ. Nanoscale topography modulates corneal epithelial cell migration. Journal of Biomedical Materials Research Part A. 2005; 75A:603–11. [PubMed: 16106433]
31. Shin S-J, Park J-Y, Lee J-Y, Park H, Park Y-D, Lee K-B, Whang C-M, Lee S-H. “On the fly” continuous generation of alginate fibers using a microfluidic device. Langmuir. 2007; 23:9104–8. [PubMed: 17637008]
32. Fukuda J, Khademhosseini A, Yeo Y, Yang X, Yeh J, Eng G, Blumling J, Wang C-F, Kohane DS, Langer R. Micromolding of photocrosslinkable chitosan hydrogel for spheroid microarray and co-cultures. Biomaterials. 2006; 27:5259–67. [PubMed: 16814859]
33. Suh KY, Seong J, Khademhosseini A, Laibinis PE, Langer R. A simple soft lithographic route to fabrication of poly(ethylene glycol) microstructures for protein and cell patterning. Biomaterials. 2004; 25:557–63. [PubMed: 14585705]
34. Talei Franzesi G, Ni B, Ling Y, Khademhosseini A. A controlled-release strategy for the generation of cross-linked hydrogel microstructures. Journal of the American Chemical Society. 2006; 128:15064–5. [PubMed: 17117838]
35. Feinberg AW, Parker KK. Surface-initiated assembly of protein nanofabrics. Nano Letters. 2010; 10:2184–91. [PubMed: 20486679]
36. Rowley JA, Madlambayan G, Mooney DJ. Alginate hydrogels as synthetic extracellular matrix materials. Biomaterials. 1999; 20:45–53. [PubMed: 9916770]
37. Shachar M, Tsur-Gang O, Dvir T, Leor J, Cohen S. The effect of immobilized RGD peptide in alginate scaffolds on cardiac tissue engineering. Acta biomaterialia. 2011; 7:152–62. [PubMed: 20688198]
38. Perka C, Spitzer R-S, Lindenhayn K, Sittinger M, Schultz O. Matrix-mixed culture: New methodology for chondrocyte culture and preparation of cartilage transplants. Journal of Biomedical Materials Research. 2000; 49:305–11. [PubMed: 10602062]
39. Liu W, Griffith M, Li F. Alginate microsphere-collagen composite hydrogel for ocular drug delivery and implantation. J Mater Sci: Mater Med. 2008; 19:3365–71. [PubMed: 18545941]
40. Kim G, Ahn S, Kim Y, Cho Y, Chun W. Coaxial structured collagen-alginate scaffolds: fabrication, physical properties, and biomedical application for skin tissue regeneration. Journal of Materials Chemistry. 2011; 21:6165–72.
41. Scheraga HA. The thrombin–fibrinogen interaction. Biophysical Chemistry. 2004; 112:117–30. [PubMed: 15572239]

42. Tønnesen HH, Karlsen J. Alginate in drug delivery systems. Drug development and industrial pharmacy. 2002; 28:621–30. [PubMed: 12149954]
43. Safi S, Morshed M, Hosseini Ravandi S, Ghiaci M. Study of electrospinning of sodium alginate, blended solutions of sodium alginate/poly (vinyl alcohol) and sodium alginate/poly (ethylene oxide). Journal of applied polymer science. 2007; 104:3245–55.
44. Boateng SY, Lateef SS, Mosley W, Hartman TJ, Hanley L, Russell B. RGD and YIGSR synthetic peptides facilitate cellular adhesion identical to that of laminin and fibronectin but alter the physiology of neonatal cardiac myocytes. American Journal of Physiology - Cell Physiology. 2005; 288:C30–C8. [PubMed: 15371257]
45. Krammer A, Craig D, Thomas WE, Schulten K, Vogel V. A structural model for force regulated integrin binding to fibronectin's RGD-synergy site. Matrix Biology. 2002; 21:139–47. [PubMed: 11852230]
46. Vogel V. Mechanotransduction Involving Multimodular Proteins: Converting Force into Biochemical Signals. Annual Review of Biophysics and Biomolecular Structure. 2006; 35:459–88.
47. Markowski MC, Brown AC, Barker TH. Directing epithelial to mesenchymal transition through engineered microenvironments displaying orthogonal adhesive and mechanical cues. Journal of Biomedical Materials Research Part A. 2012; 100A:2119–27. [PubMed: 22615133]
48. Nakaoka R, Hirano Y, Mooney D, Tsuchiya T, Matsuoka A. Study on the potential of RGD- and PHSRN-modified alginates as artificial extracellular matrices for engineering bone. J Artif Organs. 2013:1–10. [PubMed: 23456197]
49. Feinberg AW, Alford PW, Jin H, Ripplinger CM, Werdich AA, Sheehy SP, Grosberg A, Parker KK. Controlling the contractile strength of engineered cardiac muscle by hierarchal tissue architecture. Biomaterials. 2012; 33:5732–41. [PubMed: 22594976]
50. Smith JD, Chen A, Ernst LA, Waggoner AS, Campbell PG. Immobilization of Aprotinin to Fibrinogen as a Novel Method for Controlling Degradation of Fibrin Gels. Bioconjugate Chemistry. 2007; 18:695–701. [PubMed: 17432824]
51. Ahmed TA, Dare EV, Hincke M. Fibrin: a versatile scaffold for tissue engineering applications. Tissue Engineering Part B: Reviews. 2008; 14:199–215. [PubMed: 18544016]
52. Lee KY, Mooney DJ. Hydrogels for tissue engineering. Chemical reviews. 2001; 101:1869–80. [PubMed: 11710233]
53. Kleinman HK, Martin GR. Matrigel: Basement membrane matrix with biological activity. Seminars in Cancer Biology. 2005; 15:378–86. [PubMed: 15975825]
54. Lin F, Ren XD, Pan Z, Macri L, Zong WX, Tonnesen MG, Rafailovich M, Bar-Sagi D, Clark RA. Fibronectin growth factor-binding domains are required for fibroblast survival. J Invest Dermatol. 2011; 131:84–98. [PubMed: 20811396]
55. Sun Y, Duffy R, Lee A, Feinberg AW. Optimizing the Structure and Contractility of Engineered Skeletal Muscle Thin Films. Acta biomaterialia. 2013
56. Strand BL, Mørch YA, Espevik T, Skjåk-Bræk G. Visualization of alginate poly-L-lysine alginate microcapsules by confocal laser scanning microscopy. Biotechnology and Bioengineering. 2003; 82:386–94. [PubMed: 12632394]
57. Schneider CA, Rasband WS, Eliceiri KW. NIH Image to ImageJ: 25 years of image analysis. Nat Methods. 2012; 9:671–5. [PubMed: 22930834]

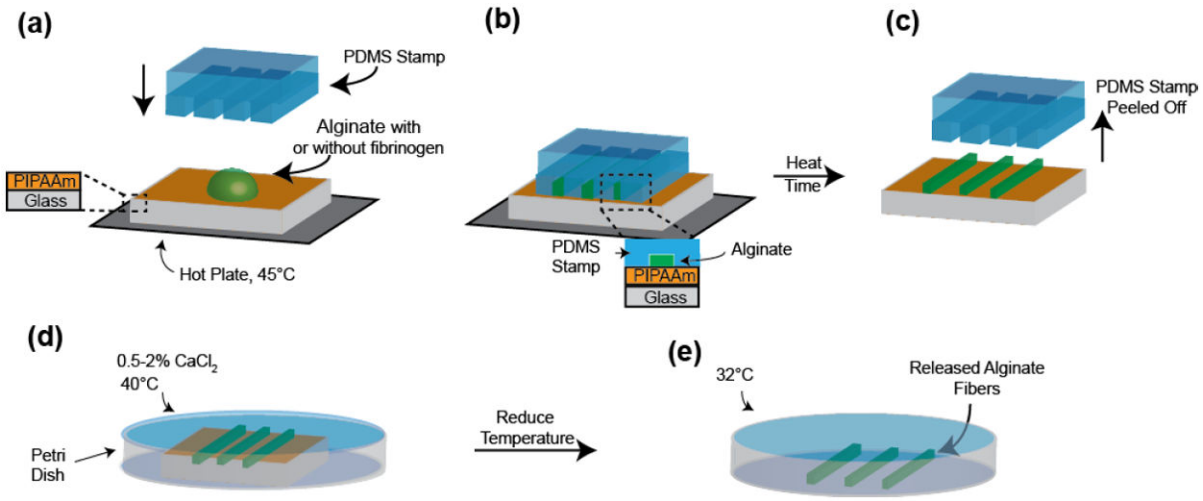

Figure 1. A schematic of the alginate microfiber and microstructure fabrication process

(a) A microfabricated PDMS stamp is pressed onto an alginate or alginate-fibrinogen drop on a PIPAAm coated coverslip. This is performed on a hotplate set to 45 °C to prevent dissolution of the PIPAAm layer. (b) The alginate is heated with the PDMS stamp in conformal contact to dry the alginate onto the PIPAAm surface. (c) Removal of the PDMS stamp yields the formation of dried, micromolded alginate microfibers. (d) The alginate fibers and structures are hydrated in a 40 °C $CaCl_2$ solution. If desirable, cells are also seeded at this step. (e) Cooling the solution below the LCST of PIPAAm (32 °C) causes the dissolution of the PIPAAm layer and the release of assembled alginate microfibers and microstructures.

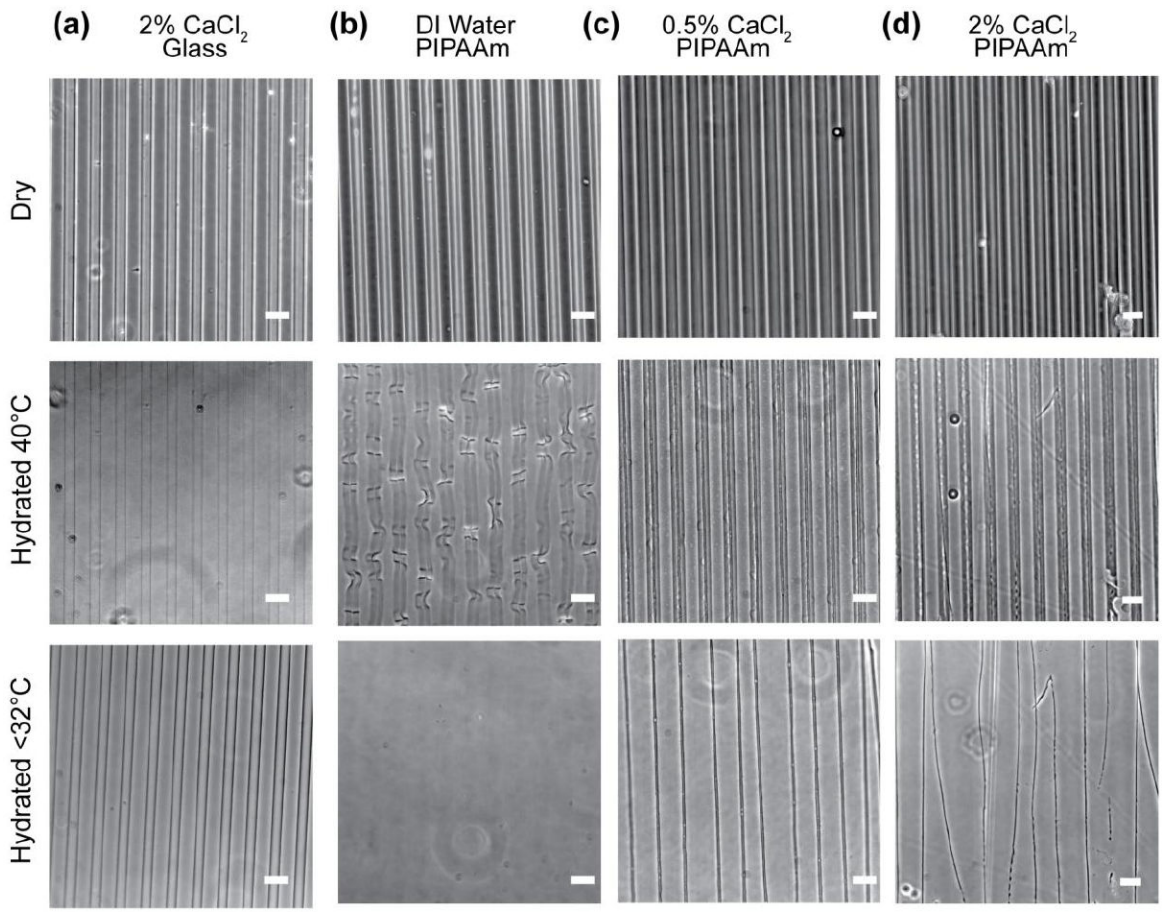

Figure 2. $CaCl_2$ and PIPAAm are necessary for the release of freestanding, assembled alginate microfibers

(a) When alginate was micromolded onto a glass surface, hydration in a 2% $CaCl_2$ solution enabled the alginate to crosslink, but the resultant fibers remained permanently bound to the glass surface. (b) Alternatively, alginate fibers that were micromolded onto a PIPAAm surface and hydrated with just DI water failed to crosslink and ultimately dissolved into solution. (c) $CaCl_2$ concentrations as low as 0.5% were sufficient to crosslink the alginate and produce microfibers upon dissolution of PIPAAm. (d) A higher concentrations of 2% $CaCl_2$ also effectively crosslinked the alginate microfibers. Scale bars are 50 μm.

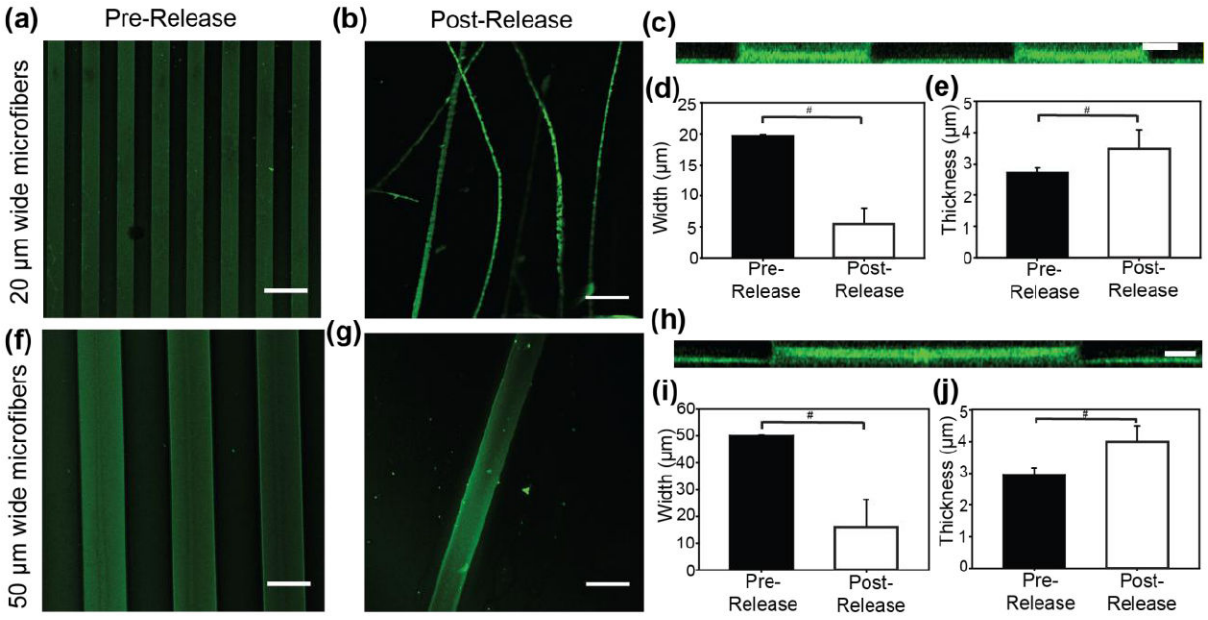

Figure 3. Alginate microfibers have tunable morphology based on the PDMS stamp used for micromolding

Confocal imaging of fluorescently-labeled alginate was used to analyze 20 µm wide fibers micromolded onto the PIPAAm surface (a) before and (b) after hydration and release into a 2% $CaCl_2$ solution. (c) A representative cross-sectional view of the 20 µm wide fibers pre-release. (d) Quantification of microfiber width pre- and post-release from the PIPAAm layer demonstrates that microfibers were initially uniform with a width of 19.71 ± 0.19 µm pre-release and decreased to a width of 5.45 ± 2.58 µm post-release (n = 40). (e) The thickness increased from 2.72 ± 0.17 µm pre-release to 3.48 ± 0.61 µm post-release (n = 12). (f) Repeating this with 50 µm wide fibers shows (f) before and (g) after hydration and release into a 2% $CaCl_2$ solution. (h) A representative cross-sectional view of the 50 µm wide fibers pre-release. (i) The alginate microfibers had a width of 50.00 ± 0.22 µm pre-release that decreased to a width of 15.79 ± 10.42 µm post-release. (j) Similar to the 20 µm wide microfibers, the thickness increased upon release from 2.96 ± 0.21 µm to 4.00 ± 0.51 µm. Scale bars are (a, b, f, g) 50 µm and (c and h) 5 µm. The symbol '#' denotes a statistically significant difference with $P<0.01$.

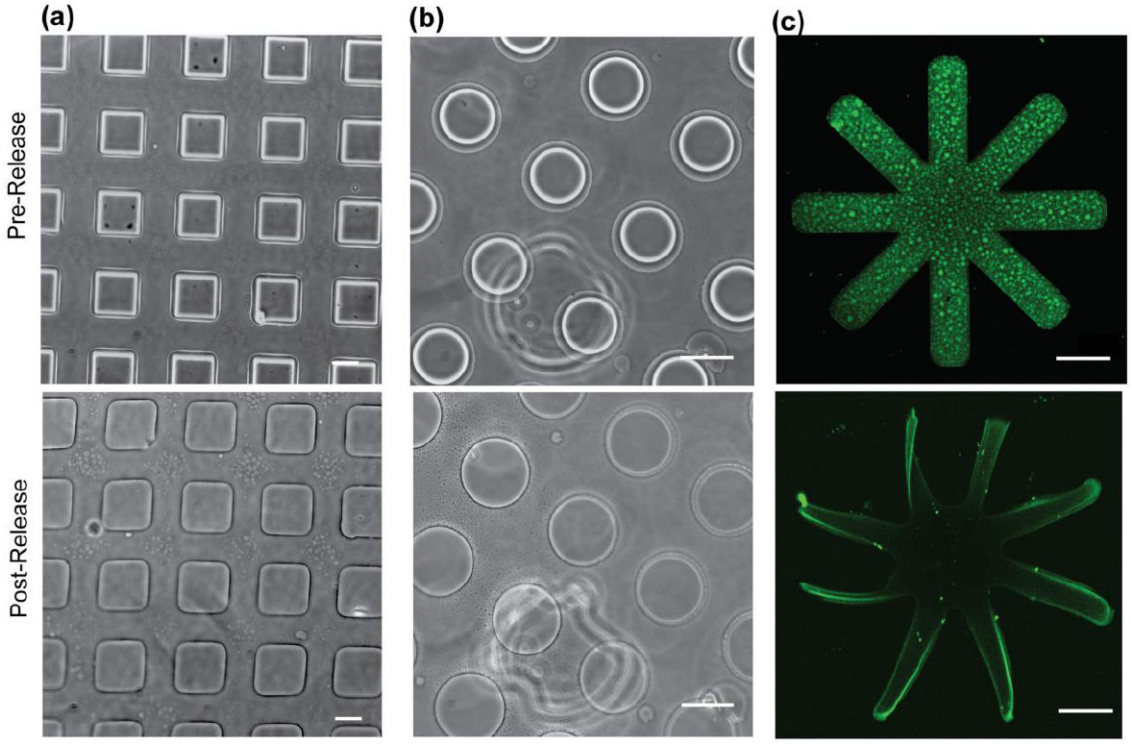

Figure 4. Fabricating freestanding, complex alginate structures

(a) An alginate sheet with 75 μm wide square pores and (b) 50 μm wide circular pores could be micromolded and thermally released while retaining their connectivity, spatial arrangement, and shape. (c) Similarly, complex structures such as a multi-arm star could be micromolded and released and retained their geometry. Scale bars are 50 μm.

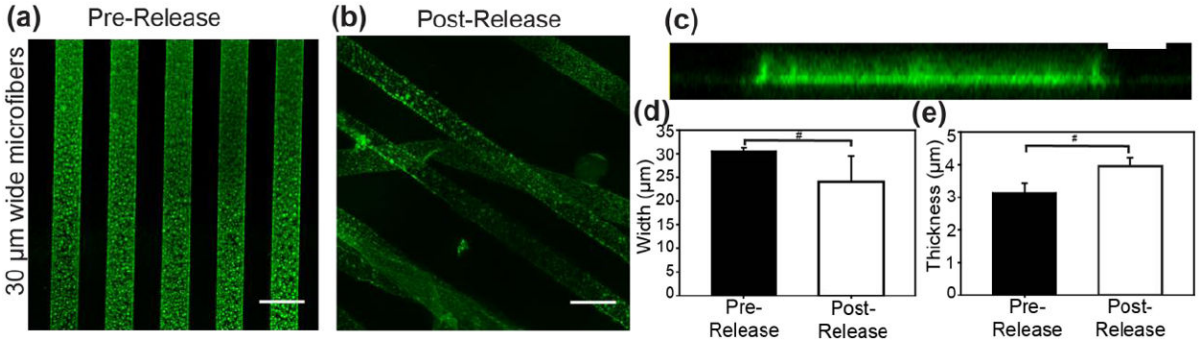

Figure 5. Quantification of alginate-fibrin microfiber morphology

Confocal imaging of fluorescently labeled alginate was used to analyze 30 μm wide alginate-fibrin microfibers (a) before and (b) after hydration and release into a 2% $CaCl_2$ and 10 U/ml thrombin solution. (c) A representative cross-sectional view of a 30 μm wide fiber pre-release. (d) The microfibers were initially uniform with a width of 30.48 ± 0.94 μm pre-release and decreased to a width of 24.10 ± 5.44 μm post-release (n = 29). (e) The thickness increased from 3.14 ± 0.29 μm pre-release to 3.96 ± 0.25 μm post-release (n = 11). Scale bars are (a) and (b) 50 μm and (c) 5 μm. The symbol '#' denotes a statistically significant difference with $P<0.001$.

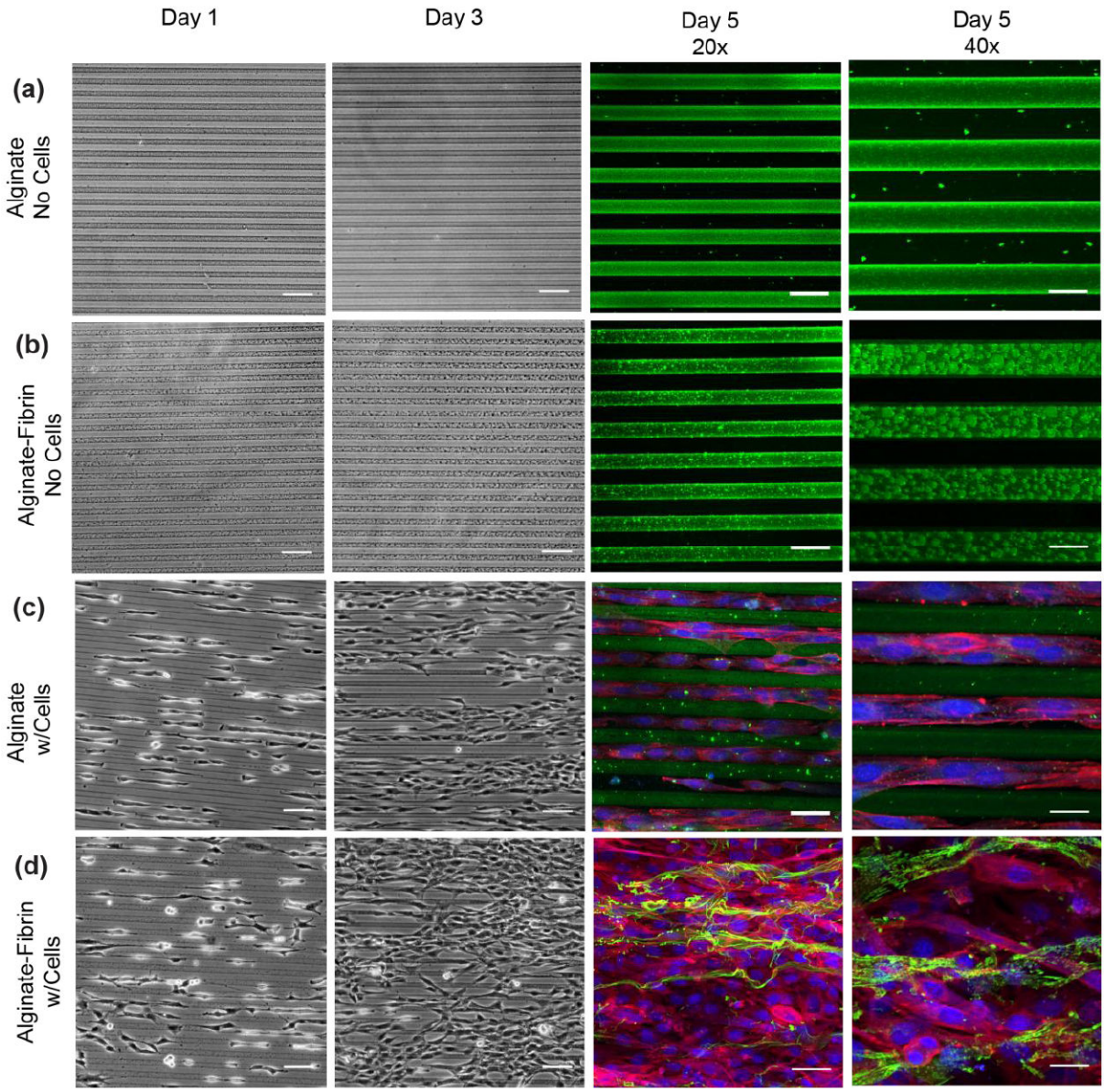

Figure 6. Determining the stability of alginate and alginate-fibrin microfibers over time in physiological solution with and without cells

(a) Alginate and (b) alginate-fibrin microfibers were micromolded onto a glass substrate and kept in growth medium for 5 days. In both cases, the microfibers remained intact. Unlike the pure alginate microfibers, the alginate-fibrin microfibers had a textured appearance. (c) Alginate microfibers were also micromolded onto a glass substrate and seeded with 10^5 C2C12 cells. After 5 days in culture, fluorescent imaging demonstrated that the alginate fibers remained intact in the original micromolded form. Cells instead adhered to the glass region in-between the alginate microfibers and aligned parallel to the length of the microfibers. (d) Alginate-fibrin microfibers were also micromolded onto a glass substrate and seeded with 10^5 C2C12 cells. After 5 days in culture, the cells were able to degrade and rearrange the alginate-fibrin microfibers. Scale bars are 100 μm for all day 1 and day 3

images, 50 μm for all day 5 20x images, and 25 μm for all day 5 40x images. Cells are labeled for nuclei (blue) and actin filaments (red) and the alginate is fluorescently labeled (green).

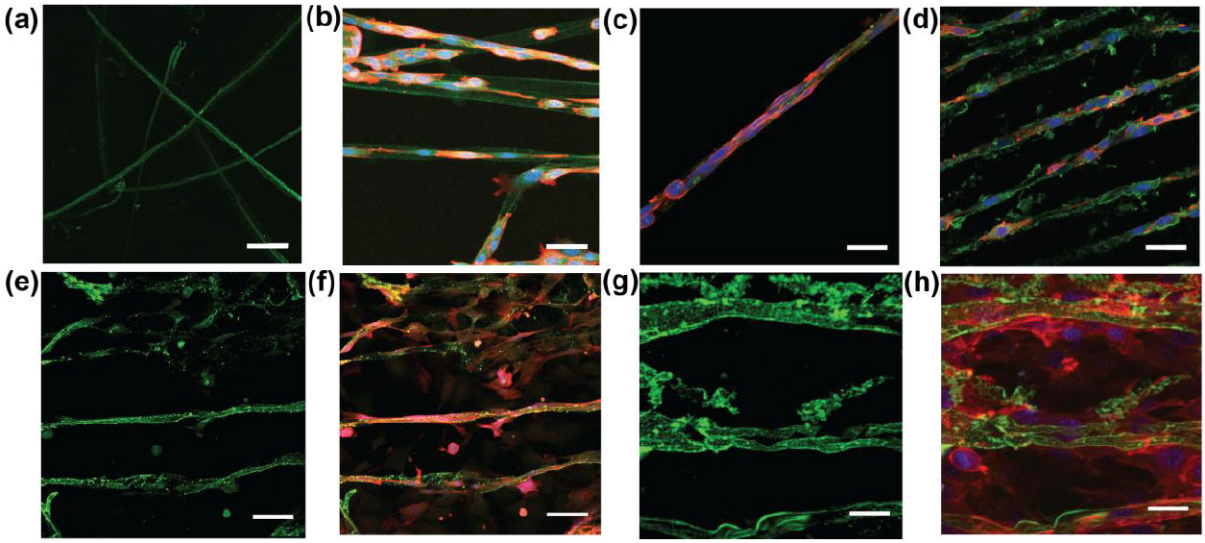

Figure 7. Fabricating alginate-fibrin microfibers to control cell adhesion and alignment

C2C12 myoblasts were seeded on fluorescently-labeled, micromolded alginate fibers while still attached to the PIPAAm surface and cultured for 12 hours. (a) The alginate fibers were unable to bind cells as indicated by the lack of adherent cells once released from the PIPAAm surface. (b) Cells remained adherent when alginate-fibrin microfibers were micromolded on PIPAAm and then released. Fluorescence imaging demonstrated that the bioactive alginate-fibrin fibers not only promoted adhesion but also influence cell alignment along (c) a single microfiber or (d) along multiple parallel fibers to yield an overall cell alignment within the freestanding construct. To assess the stability of the alginate-fibrin microfibers over a longer period, C2C12 myoblasts were seeded on micromolded alginate-fibrin microfibers and cultured for 3 days. Fluorescent imaging of the microfibers at (e) 20x and (g) 40x magnification indicated that the fibers, while slightly degraded, were still able to properly release from the PIPAAm surface. (f, h) After 3 days, the cells also remained adherent and aligned along the length of the microfibers. Cells were labeled for nuclei (blue), actin filaments (red), and the alginate was fluorescently labeled (green). Scale bars are (a) to (e) 50 μm and (g) and (h) 25 μm.